Dependence of Viscoelastic Flow Functions on Molecular Structure for Linear and Branched Polymers

S. Ramachandran, H. W. Gao, and E. B. Christiansen*

Department of Chemical Engineering, University of Utah, Salt Lake City, Utah 84112.

Received June 29, 1984

ABSTRACT: The flow properties were measured for concentrated n-butylbenzene solutions of well-characterized linear mono- and polydisperse polystyrene and polybutadiene, four-arm-star branched polystyrene and polybutadiene, and linear and four-arm-star branched random and block copolymers of styrene and butadiene. Concentrations varied from about 100 to 600 kg/m^3. Polymer molecular weights varied from about 3×10^4 to 2.5×10^6. The viscosity and first and second normal stress difference functions of the shear rate, $\dot\gamma$ ($\eta(\dot\gamma)$, $N_1(\dot\gamma)$, $N_2(\dot\gamma)$), and related steady-state shearing functions extending into the shear thinning region, and the unsteady shearing functions were determined in cone–plate shearing. The "zero" shear viscosity, η_0, for linear polymers in the entanglement region was proportional to the entanglement density, E, to the 3.5 power. With the exception of the block copolymers, η_0 for the branched polymers was proportional to $(gE)^{3.5}$. The ratio N_2/N_1 was −0.29 for all linear-polymer data and −0.214 for all branched-polymer data with a standard deviation of less than 2%.

Introduction

This presentation concerns the material viscometric flow functions, the viscosity shear rate functions, $\eta(\dot\gamma)$, the first and second normal stress difference functions, $N_1(\dot\gamma)$ and $N_2(\dot\gamma)$, and related functions and stress growth and decay functions. These are of theoretical and practical interest.

While many industrially important polymer flows are viscometric, most include both viscometric and nonviscometric flows. Fortunately, the kinematics for many industrially important flows are sufficiently simple that the viscometric flow functions are valid or can be considered to be approximately so. Furthermore, these viscometric flow functions are of critical importance in evaluating constitutive theory. The first and second normal stress difference functions are of special interest owing to their important effects in polymer processing and to the evidence presented herein and elsewhere[14,15,21] that they depend much more strongly on polymer structure than the viscosity functions.

Extensive data have been reported on the dependence of $\eta(\dot\gamma)$ on polymer structure and shearing conditions for polymer solutions and melts[15]. Similar but less extensive data have been reported for $N_1(\dot\gamma)$ (e.g., ref 15 and 27). However, trustworthy data for $N_2(\dot\gamma)$ are relatively scarce owing largely to the difficulty in experimentation, but to some extent to the belief that it is negligibly small.

The principal objective of this present study was to elucidate $N_2(\dot\gamma, M, \mathrm{MWD}, \mathrm{branching})$. However, the corresponding dependencies for η and N_1 were simultaneously determined. The second normal stress difference generates forces which tend to center the wire in wire coating;[34] it is suggested to be important in journal bearing theory;[19a] it promotes particle translational motion, e.g., migration away from the wall in tube flow,[20] and it controls particle orbits or orientation in particle motion through viscoelastic fluids.[20] Several flow instabilities have been shown to be sensitive to the magnitude of N_2 or the ratio $\psi = N_2/N_1$ (e.g., ref 25 and 29). Furthermore, $N_2(\dot\gamma)$ is of importance in the development and evaluation of continuum and molecular models.[4,28,38]

Second normal stress difference data are usually reported in terms of the ratio $\psi = N_2/N_1$. Most reported experimental values of $-\psi$ range from 0.0 (the Weissenberg hypothesis value) to about 0.4 for polymer melts and solutions (e.g., ref 22 and 35). However, values as high as near 0.6 have been reported for a poly(methyl methacrylate) melt.[18] Some of the variations in the results are a consequence of weaknesses in experimental methods and data analyses. Theoretical relationships such as the continuum corotational models (e.g., ref 3) and others (e.g., ref 36) predict values up to 0.5, and there are empirical–theoretical arguments for 0.5 as a maximum.[4,29] Predictions of structural models vary considerably, but those of particular interest are low ("zero") $\dot\gamma$ range predictions of $\psi = -^2/_7$ for linear molecules by the Doi and Edwards reptation model[10] and the prediction of the Curtiss–Bird development for linear narrow MWD molecules, $\psi = -^2/_7(1 - \epsilon)$.[7]

Methods for the accurate determination of the viscosity, η, for polymer solutions and melts are well-known and well documented as are methods for the determination of N_1 (e.g., ref 3, 8, 12, and 37). The first normal stress difference, N_1, is commonly and quite accurately determined from the total normal force generated in cone–plate shearing. Numerous methods have been proposed for the determination of the second normal stress difference, N_2 (e.g., ref 3, 8, 12, and 37). However, the method potentially most reliable is probably cone–plate shearing with instrumentation for plate pressure distribution measurements. However, cone–plate measurements are limited to low shear rates, i.e., usually $<10^3$ s^{-1}, by flow instabilities, etc., depending on the shearing geometry and viscoelastic properties of the material. Although many methods for higher shear rate measurements have been proposed (e.g., ref 3, 8, 12, and 37), the reliability of such measurements has not been established[5,37] although some believe that some hole-error methods can now yield acceptable results (e.g., ref 21).

Among the major sources of experimental difficulties are viscous heating, end or edge effects in tube and cone–plate measurements, respectively, and hole errors in pressure tap measurements. (See, e.g., ref 33 and 37 for a complete discussion of difficulties and means of coping.)

Experimental Section

The polymers[13,14,30,31] included well-characterized mono- and polydisperse linear polystyrenes ($M_w = 37 \times 10^3$–2×10^6; $M_w/M_n < 1.06$–22.0), monodisperse four-arm-star branched polystyrenes ($M_w = 110 \times 10^3$–2.4×10^6; $M_w/M_n < 1.06$), four-arm-star polybutadienes ($M_w = 300 \times 10^3$ and 330×10^3; $M_w/M_n = 1.78$), four-arm-star random and block styrene–butadiene copolymers ($M_w = (130$–$350) \times 10^3$; $M_w/M_n = 1.30$–1.94), and one uncharacterized sample of linear polybutadiene. Concentrations varied from about 100 to 600 kg/m^3 in n-butylbenzene but a 450 kg/m^3 solution of linear polystyrene in tricresyl phosphate was included.

The viscometric flow functions were determined in cone–plate shearing with a stiffened R-17 Weissenberg rheogoniometer.[32] The common diameter of the cone and plate was 74 mm; and the cone

0024-9297/85/2218-0695$01.50/0

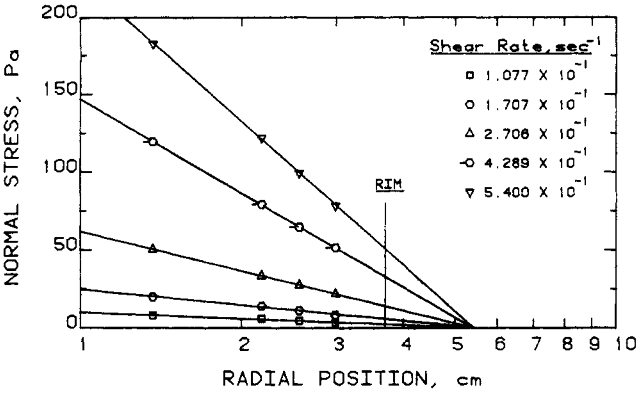

Figure 1. Total local pressure on the plate relative to atmospheric pressure vs. radial position for a 300.0 kg/m^3 solution of a four-arm-star branched polybutadiene in *n*-butylbenzene (M_w = 300000, M_w/M_n = 1.77).

angles used were $^1/_2$°, 2°, 4°, and 6° (the 6° cone was used in some unsteady shearing studies). Plate pressure distributions were determined by four rapid response capacitive pressure transducers mounted with their 2.5 mm o.d. diaphragms flush with the plate. In the more recent research,[30] essentially point plate pressures could be resolved to within as little as 0.5–1.0 Pa and less. The shear rate range was limited at the low end by instrumental sensitivities and at the high limit by flow instabilities. The temperature was controlled at 25 ± 0.1 °C. Our innovation of the use of flush mounted miniature pressure transducers with very low response times (e.g., ref 14 and 26) makes possible for the first time the simultaneous and accurate determination of N_1 and N_2 in unsteady as well as steady shearing modes.

Data Analysis

The usual relations were employed in the data analysis:

$$\dot{\gamma} = -\Omega/\alpha \tag{1}$$

$$\eta(\dot{\gamma}) = -\tau/\dot{\gamma} = 3T\alpha/2\pi R^3\Omega \tag{2}$$

$$N_1(\dot{\gamma}) = \Pi_{11} - \Pi_{22} = -2F/\pi R^2 \tag{3}$$

$$N_2(\dot{\gamma}) = \Pi_{22} - \Pi_{33} = \Pi_{22}(R) \tag{4}$$

$$\frac{\partial \Pi_{22}(r)}{\partial \ln r} = (\Pi_{11} - \Pi_{22}) + 2(\Pi_{22} - \Pi_{33}) \tag{5}$$

$$\psi_1(\dot{\gamma}) = -N_1(\dot{\gamma})/\dot{\gamma}^2 \tag{6}$$

$$\psi_2(\dot{\gamma}) = -N_2(\dot{\gamma})/\dot{\gamma}^2 \tag{7}$$

$$\psi = N_2/N_1 = \psi_2/\psi_1 \tag{8}$$

$$J(\dot{\gamma}) = \psi_1/2\eta^2 \tag{9}$$

$$R_i = R\exp[-\psi/(1 + 2\psi)] \tag{10}$$

These relations are based on ideal shearing flow. Corrections must be made if the effects of deviations are not negligible. Derivations with assumptions, definitions, and sign convention are given in ref 3 except that eq 10 is derived in ref 31.

Results

Typical plate pressure distribution data are shown in Figure 1. The Π_{22} vs. ln *r* functions are linear as predicted by eq 5 and have a common abscissa intercept. Both N_1 and N_2 can be computed from the slopes of these lines and the total normal force by eq 3 and 5, the slope–total force, or ST, method. Alternatively, these can be determined from the slopes and the rim intercepts at **R** by eq 4 and 5, the slope–rim, or SR, method. By eq 10, the common abscissa intercept indicates that, for these data, ψ is independent of $\dot{\gamma}$, the general observation. The typical flow functions presented in Figure 2 extend from the zero shear rate into the shear thinning region and again show that for these data $\psi \neq f(\dot{\gamma})$. It will be noted that coefficients determined by the slope–total force, the ST method, and by the slope–rim, the SR method, agree very well—usually within ±1%. Also, data obtained with 2° and 4° cones agree within ±2%. The ratios $\psi = N_2/N_1$ for the linear polystyrenes and the linear polybutadiene are shown in Figure 3 as a function of $\dot{\gamma}$. The data are within about ±5% of ψ = –0.287. The average $-\psi$ for each sample, including the solution of linear polystyrene in tricresyl phosphate, is near the average for all of the samples. There is no definite segregation by method of calculation or sample. Over the range of variables studied, ψ appears to be independent of solvent, concentration, molecular weight, and molecular weight distribution, in addition to being independent of $\dot{\gamma}$, and is essentially the same for polybutadiene as for polystyrene. While the Doi–Edwards reptation model prediction, $\psi^0 = -^2/_7$, is almost identical with the observed average for the linear polymer solutions, both the Doi–Edwards and Curtiss–Bird relations predict ψ to vary with shear rate, in disagreement with our data. While our data do not extend to particularly high shear rates, a significant decrease predicted by the Doi–Edwards relation was not observed. However, the reptation theory does predict that if the number of entanglements per chain is sufficiently high, ψ_1 for linear polymers is independent of concentration, molecular weight, and molecular weight distribution.[9] A recent study is of interest in which three methods for the determination of N_2 are compared and

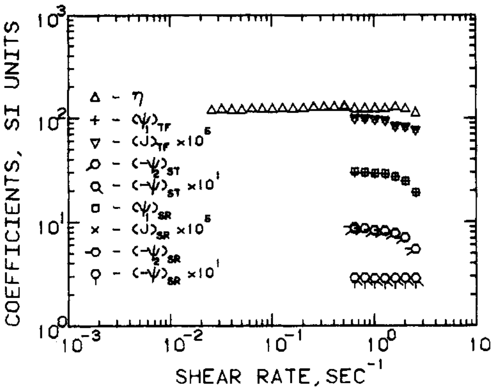

Figure 2. Steady shear data for a 400.0 kg/m^3 solution of polystyrene in *n*-butylbenzene (M_w = 272000; M_n = 113,000; M_w/M_n = 2.41): $()_{TF}$ determined from total normal force on plate relation 3; $()_{ST}$ determined by slope–total normal force method, relations 3 and 5; $()_{SR}$ determined by slope–rim method, relations 4 and 5.

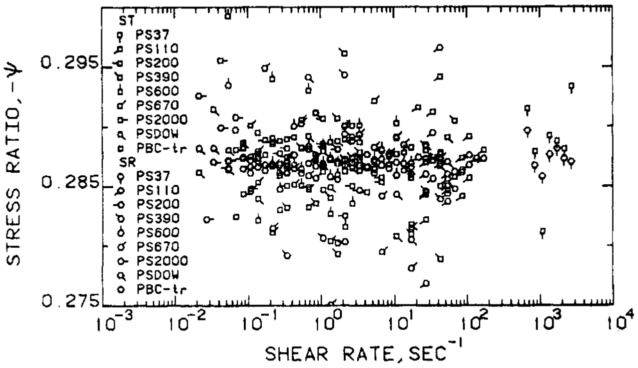

Figure 3. Ratio of N_2 to N_1 as a function of shear rate for concentrated solutions of linear polystyrenes and polybutadienes: (ST) slope–total force and (SR) slope–rim methods of pressure distribution data analysis.

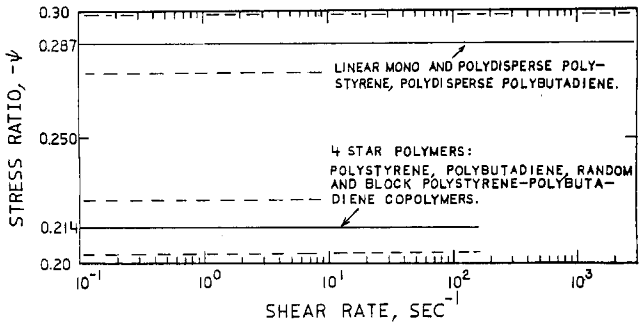

Figure 4. Comparison of all normal stress difference data: (---) deviation limits.

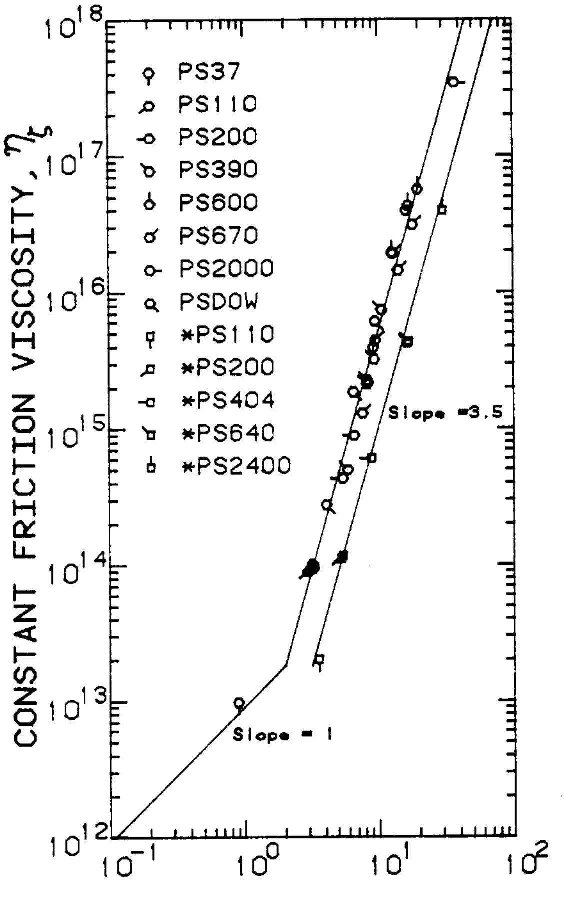

Figure 5. Constant friction viscosity vs. entanglement density for concentrated solutions of linear and four-star branched polystyrenes in *n*-butylbenzene. The asterisks identify four-arm-star branched polystyrene polymers.

a value of $\psi = -0.31 \pm 0.05$ was reported for a 7.14% solution of a linear polystyrene in a solution of tricresyl phosphate and Aroclors.[19b]

In Figure 4, a line representing the average ψ for all of the four-arm-star branched samples is compared with the corresponding line for all of the linear polymers. The average ψ's for the four-arm-star polystyrene and polybutadiene solutions were −0.214 and −0.216, respectively. All of the data are within about ±5% of the average. Thus, for the four-arm-star polymer solutions, ψ appears to be independent of molecular weight, molecular weight distribution, and concentration and is essentially the same for the polystyrenes, polybutadienes, and the random and block copolymers. The distinct difference between ψ for the four-arm-star and ψ for the linear polymers is well outside the experimental error. While our data are in the range of reported data for polymer solutions and melts (e.g., ref 2, 19b, 22, and 35), they are unique in being sufficiently definitive to demonstrate the distinct effect of branching. The reptation theory predicts that ψ is the same for star and linear polymers.[9]

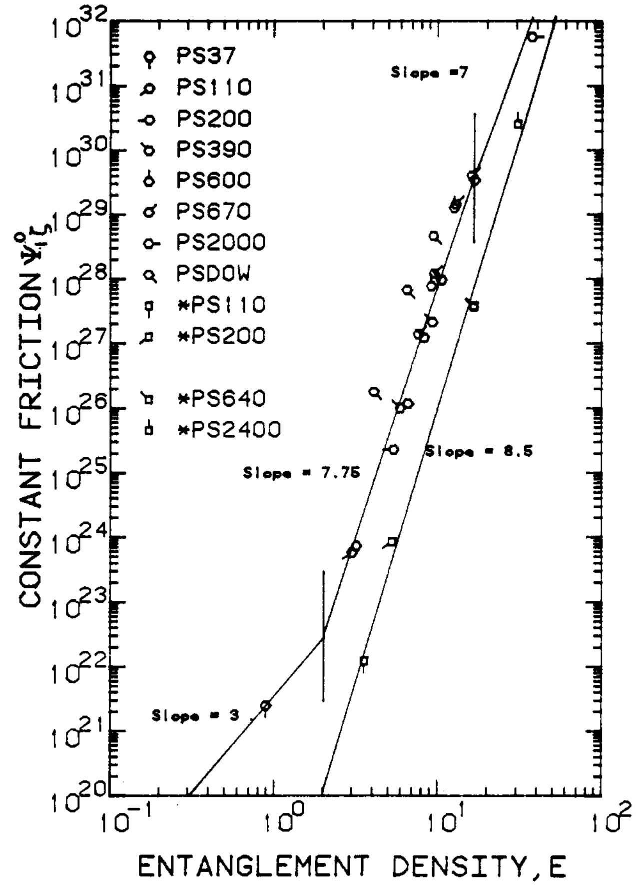

Figure 6. Constant-friction first normal stress difference coefficient vs. entanglement density E for concentrated solutions of linear and four-star-branched polystyrenes.

As indicated in Figure 5, in the entanglement density range ($E > 2$) the constant friction zero shear viscosities for both the branched and linear polystyrenes, including one polydisperse polystyrene ($M_w/M_n = 2.41$), are proportional to $(E)^{3.5}$ (or, equivalently, $(CM)^{3.5}$) in agreement with most previous results.[15,39] The constant friction viscosity was determined by computing, by means of η_0 and the WLF relation, a glass transition solution viscosity and correcting it to the pure polymer glass temperature.[23b] The use of η_ζ tends to isolate the effect of structure. As predicted by Bueche,[6] $(\eta_0)_B/(\eta_0)_L \propto (g)^{3.5}$. For the star branched 28% and 38% styrene block styrene–butadiene copolymers, η_0 was proportional to $(M_w)^{5.5}$ and $(M_w)^{>6}$, respectively, whereas for the random copolymers, the exponent was 3.2. The higher exponents probably reflect the strength of the network formed by the dispersed phase polystyrene domains.

According to Figure 6, $\psi_{1\zeta}{}^0 \propto E^{7.0\text{ to }7.8}$, ($\psi_1{}^0 \propto (CM^{7.0\text{ to }7.8})$ for linear polymers ($E > 2$) in agreement with previous results for many polymer solutions and melts wheras for the branched-polymer solutions $\psi_\zeta{}^0 \propto E^{8.5}$. Since the ratio $\psi = \psi_2/\psi_1 = N_2/N_1$ is independent of M and concentration, $\psi_{2\zeta}{}^0$ (or $\psi_2{}^0$) will have the same dependency on E (or CM) as $\psi_{1\zeta}{}^0$ but will be smaller by the ratio ψ.

The steady-state shear compliance, $J(\dot{\gamma})$, increases, beginning approximately with the onset of shear thinning for the monodisperse linear- and branched-polymer solutions (see Figure 2) and decreases (ψ decreases with increase in

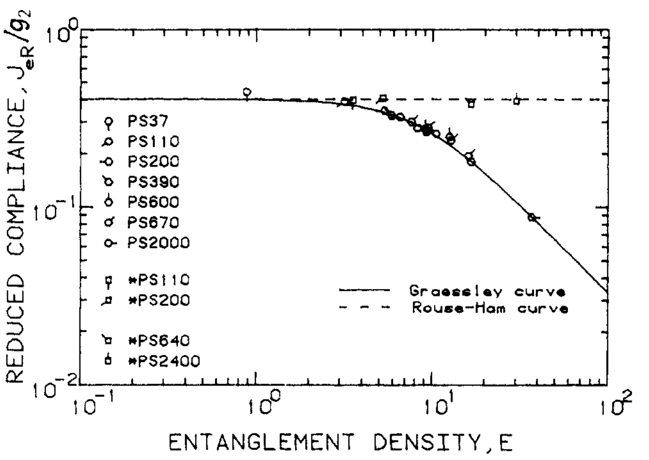

Figure 7. Reduced steady-state compliance, J_{eR}/g_2, vs. the entanglement density, E, for monodisperse linear and four-arm-star branched polystyrene solutions in n-butylbenzene. The asterisks (*) identify four-arm-star branched polystyrene solutions.

$\dot{\gamma}$ faster than η^2) beginning with the onset of shear thinning in the case of the polydisperse polymer solutions[13,30] as reported by others.[15]

The steady-state zero shear rate compliance, $J_e^0 = \psi_1^0/(2\eta_0^2)$, for the linear polymers increased proportional to M at low entanglement densities, as predicted by the Rouse relation as adapted for concentrated solutions (ref 12, p 232), $J_e^0 = 0.4M/CRT$, and became independent of M at entanglement densities >20. The critical M_c' was approximately $8.3M_e$ in agreement with predictions.[15] The J_e^0 for solutions of linear polydisperse polystyrene were higher than those for the monodisperse solutions by a factor $(M_z/M_w)^d$, where d increased from 2.5 to 3.5 for a change in concentration from 250 to 580 kg/m^3.[30] In the initial research,[13,14] d was 3.5 for 450 kg/m^3 solutions of linear polydisperse polystyrene in n-butylbenzene.

The dependence of J_{eR} on E for linear polymers is in agreement with an empirical relation by Graessley[15] (Figure 7) and the four-star, branched-polymer solution data are well represented by the Rouse–Ham relation,[17] $(J_e^0)_B = 0.4g_2M/CRT$, as has been found by others for concentrated solutions and melts (e.g., ref 16 and 39). This proportionality to M for star branched polymers is predicted by Doi and Kuzuu.[11] Some experimental data suggest that $(J_e^0)_B$ becomes independent of M at quite high M but this is controversial (e.g., Masuda et al.,[24] Graessley and Roovers,[17] Ferry[12] (e.g., p 386)). At low E, J_e^0 is proportional to C^{-1}; and at high E, to C^{-2} in agreement with data for other systems.

Transducer pressure data during stress growth following the sudden onset of shearing or during stress decay following the abrupt termination of shearing, when normalized relative to the steady-state shearing values, superimpose as illustrated in Figures 8 and 9. We have observed such superposition for both mono and polydisperse samples,[14,23a] including cases with stress growth "overshoot".[23a] However, others[1] have not observed such superposition during normal stress decay for a polydisperse polyisobutylene solution but did report such superposition for a monodisperse polystyrene solution. On the basis of rather limited data, relaxation occurs more rapidly the higher the steady-state shear rate and the lower the M and the MWD as might be expected. However, of particular interest, such superposition indicates that the first and second normal stress differences grow and decay at the same relative rates and that the N_1 and N_2 relaxation processes are similar. Constitutive theory should account for these observations.

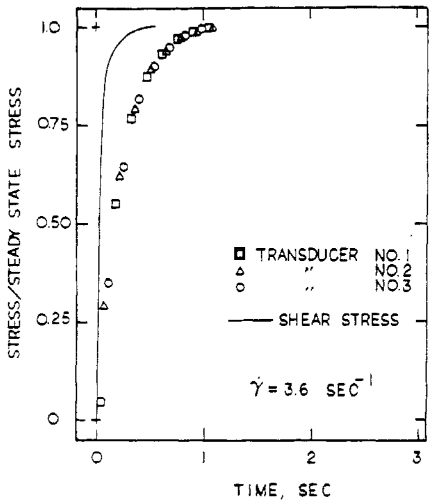

Figure 8. Shear and normal stress growth data for the 60 wt % polydisperse polystyrene solution (M_w = 77770, M_w/M_n = 22).

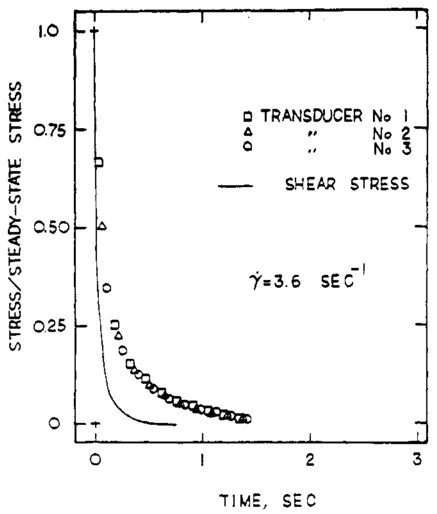

Figure 9. Shear and normal stress decay data for the 60 wt % polydisperse polystyrene solution (M_w = 77700, M_w/M_n = 22).

Conclusions

Among the more interesting conclusions for the polymer solutions and variable ranges studied are the following:

(1) The sign of the first normal stress difference is opposite that of the second in agreement with all of our previous results and the opinion of most others in the field.

(2) The ratio ψ for the linear polymers, −0.287, is distinctly different from that for four-arm-star branched polymers, −0.214.

(3) The ratio ψ is independent of concentration, molecular weight, molecular weight distribution, shear rate, the polymer composition, and perhaps the solvent. Also, ψ has the same numerical value during stress growth and decay or relaxation as during steady-state cone–plate shearing.

(4) The basic mechanisms and relaxation processes for N_1 and N_2 appear to be similar, and constitutive theory should account for this.

Acknowledgment. We gratefully acknowledge the financial assistance of an NSF grant, the provision of samples and characterization data by Dr. L. J. Fetters, Dr. D. C. Bogue, the Phillips Petroleum Co., and the Monsanto Chemical Co., the MWD analysis by the Eastman Kodak Co., and the assistance of Mr. Grant Coon and Mr. Dwight L. Moody, Jr., of the NASA Ames Laboratory with in-

formation for the fabrication of the variable capacitance pressure transducers.

Notation

C	concentration, mass per unit volume
E	entanglement density, $CM_w/\rho M_e$
F	total normal or axial force on plate
f	number of branches in star polymer
g	mean square radii of gyration ratio, $\langle S^2\rangle_B/\langle S^2\rangle_L = (3f-2)/f^2$
g_2	$(15f-14)/(3f-2)^2$
$J_e{}^0$	steady-state zero shear compliance, $\psi_1{}^0/(2\eta_0{}^2)$
$J(\dot{\gamma})$	steady-state shear compliance, $\psi_1(\dot{\gamma})/2(\eta(\dot{\gamma}))^2$
J_{eR}	$(J_e{}^0CRT/M)[\eta_0/(\eta_0-\eta_s)]^2$
$(J_e{}^0)_B$	$0.4g_2M/CRT$ for branched polymers
M	molecular weight
MWD	molecular weight distribution
M_c	characteristic M from $\eta_0(M)$
M_e	M between entanglement loci
M_n, M_w, M_z	number-, weight-, and z-average M
N_1, N_2	first and second normal stress differences
p	pressure, isotropic
r	radial distance
R	gas constant
$\mathbf{R}$	radius of plate
$\mathbf{R}_i$	radial distance to intercept of $\Pi_{22}(\ln r)$ on abscissa for Π_{22} vs. $\ln r$ plot
T	torque
t	time

Greek Symbols

α	cone angle
$\dot{\gamma}$	shear rate
η, η_0	viscosity and zero-shear-rate viscosity
η_s	solvent viscosity
η_ζ	constant friction viscosity
ρ	polymer density
ψ	N_2/N_1 or ψ_2/ψ_1
ψ_1, ψ_2	N_1 and N_2 coefficients, $-N_1/\dot{\gamma}^2$, $-N_2/\dot{\gamma}^2$
$\psi_1{}^0$, $\psi_2{}^0$	N_1 and N_2 coefficients as $\dot{\gamma} \rightarrow 0$
$\psi_{1\zeta}{}^0$	N_1 constant friction coefficient, $2J_e{}^0\eta_{0\zeta}{}^2$
Ω	rotational velocity
π	pi
Π_{ii}	total normal stress, $p\delta + \tau_{ii}$

Registry No. Polystyrene (homopolymer), 9003-53-6; polybutadiene (homopolymer), 9003-17-2; (Butadiene)·(styrene) (copolymer), 9003-55-8.

References and Notes

(1) Attane, P.; LeRoy, P.; Pierrard, J. M.; Turrel, G. *J. Non-Newtonian Fluid Mech.* **1977/1978** *3*, 1.
(2) Baird, D. G. *Rheol. Acta.* **1980**, *19*, 183.
(3) Bird, R. B.; Armstrong, R. C.; Hassager, O. "Dynamics of Polymeric Liquids"; Wiley: New York, 1977; Vol. I.
(4) Bird, R. B.; Hassager, O.; Abdel-Khaik, S. T. *AIChE J.* **1974**, *20*, 1041.
(5) Boger, D. V.; Denn, M. M. *J. Non-Newtonian Fluid Mech.* **1980**, *6*, 163.
(6) Bueche, F. *J. Chem. Phys.* **1964**, *40*, 484.
(7) Curtiss, C. F.; Bird, R. B. *J. Chem. Phys.* **1981**, *74*, 2026.
(8) Dealy, J. M. "Rheometers for Molten Plastics"; Van Nostrand-Reinhold, New York, 1982.
(9) Doi, M. Letter to E. B. Christiansen, June 1984.
(10) Doi, M.; Edwards, S. F. *J. Chem. Society, Faraday Trans. 2*, **1979**, *75*, 38.
(11) Doi, M.; Kuzuu, N. Y. *J. Polym. Sci., Polym. Lett. Ed.* **1980**, *18*, 775.
(12) Ferry, J. D. "Viscoelastic Properties of Polymers"; Wiley: New York, 1980.
(13) Gao, H. W. Ph. D. Thesis, University of Utah, Salt Lake City, 1979.
(14) Gao, H. W.; Ramachandran, S.; Christiansen, E. B. *J. Rheol.* *25*, **1981**, 213.
(15) Graessley, W. W. *Adv. Polym. Sci.* **1974**, *16*, 1.
(16) Graessley, W. W.; Masuda, T.; Roovers, J. E. L.; Hadjichristidis, N. *Macromolecules* **1976**, *9*, 127.
(17) Graessley, W. W.; Roovers, J. E. L. *Macromolecules* **1979**, *12*, 959.
(18) Han, C. D. *Trans. Soc. Rheol.* **1974**, *18*, 163.
(19) (a) Kai, Z. *J. Non-Newtonian Fluid Mech.* **1982**, *11*, 201. (b) Keentok, M.; Tanner, R. I. *J. Rheol.* **1982**, *26*, 301.
(20) Leal, L. G. *J. Non-Newtonian Fluid Mech.* **1979**, *5*, 33.
(21) Lodge, A. S.; Vargas, L. de *Rheol. Acta* **1983**, *22*, 151.
(22) Lee, B. L.; White, J. L. *Trans. Soc. Rheol.* **1974**, *18*, 467.
(23) (a) Leppard, W. R.; Christiansen, E. B. *AIChE J.* **1975**, *21*, 999. (b) Lindeman, L. R. M.S. Thesis, Northwestern University, Evanston, IL, 1967.
(24) Masuda, T.; Ohta, Y.; Onogi, S. *Macromolecules*, **1971**, *4*, 763.
(25) McIntire, L. V.; Schowalter, W. R. *AIChE J.* **1972**, *18*, 102.
(26) Miller, M. J. Ph.D. Thesis, University of Utah, Salt Lake City, UT, 1968.
(27) Nishida, N.; Salladay, D. G.; White, J. L. *J. Appl. Polym. Sci.* **1971**, *15*, 1181.
(28) Olabisi, O.; Williams, M. C. *Trans. Soc. Rheol.* **1965**, *16*, 15.
(29) Petrie, J. S.; Denn, M. M. *AIChE J.* **1976**, *22*, 209.
(30) Ramachandran, S. Ph.D. Thesis, University of Utah, Salt Lake City, UT, 1985.
(31) Ramachandran, S.; Christiansen, E. B. *J. Non-Newtonian Fluid Mech.* **1983**, *13*, *21*.
(32) Ramachandran, S.; Christiansen, E. B. *J. Rheol.* **1980**, *24*, 325.
(33) Schowalter, W. R. "Mechanics of Non-Newtonian Fluids"; Pergamon Press: New York, 1978.
(34) Tadmor, Z.; Bird, R. B. *Polym. Eng. Sci.* **1974**, *14*, 124.
(35) Tanner, R. I. *trans. Soc. Rheol.* **1973**, *17*, 365.
(36) VanArsdale, W. E. *J. Rheol.* **1982**, *26*, 477.
(37) Walters, K. "Rheometry"; Chapman and Hall: London, 1975.
(38) Williams, M. C. *AIChE J.* **1975**, *21*, 1.
(39) Yasuda, K.; Armstrong, R. C.; Cohen, R. E. *Rheol. Acta* **1981**, *20*, 163.